Research on the Splice Breakage Monitoring System for Steel-cord Belt Conveyor

Huang Min
Mechanical & Electrical Engineering School
Beijing Information Science & Technology University
Beijing, 100192 P. R, China
Hm_cumt@sina.com

***Abstract* - A new method of monitoring and forecasting the steel-cord belt splice breakage and tension super-threshold is described in this paper, which is established on the basis of the measurement and analysis of the F-L (tensile Force-Length) characteristic curve of steel-cord belt splices. The principles and methods for monitoring the splice length and the belt tension are elaborated. And a practical real-time monitoring system is developed according to this novel method. Simulation experiments and industrial application have shown that it is of high measuring accuracy, high reliability and stability.**

Index Terms - steel-cord belt; splice breakage; monitoring

1. Introduction

The steel-cord belt is one key component of the steel-cord belt conveyor, a type of continuous transport machine widely used in many industrial areas. While the belt conveyor being in operation, the tensile force is transferred through the viscous force between the rubber and steel cords; the loads are sustained by the steel cords equally arranged in the belt. So the steel-cord belt is of high tensile strength. However, the belt usually contains many splices, which are the weakest links in the belt loop, so most of the belt breakage has happened in the splice region, which are not only affecting the production but also endangering the workers' lives. Besides, the tension super-threshold of the conveyor belt is another kind of dangerous working condition, which may directly result in splice breakage and some other failures as well. Therefore, it is of great importance to manage to prevent and avoid such failures.

Over the past decades, many measures have been applied to monitor and forecast the splice breakage and the tension super-threshold of the conveyor belt. This paper, however, depicts a new method of monitoring the above-mentioned failures and a practical real-time monitoring system developed according to this method. It has been proved by both simulation experiments and industrial application that this system is of high measuring accuracy, reliability and stability.

2. Principles of Monitoring and Diagnosing

2.1 Mechanism of the Splice Breakage

The damages of belt splices may be caused by many factors such as improper coating, incorrect pressure or pressing temperature in splicing, end corrosion of steel cords and surface laceration of the belt, etc. Nevertheless, all kinds of damages share a common characteristic, that is, the deformation of splice region increases gradually together with the development of damages and when it reaches to a certain degree, some steel cords begin to be drawn out, the more the steel cords being drawn, the larger the deformation of splice region. As a result, the viscous force between the steel cords and the rubber are continually weakened till all the steel cords are drawn out, causing a sudden breakage of the splice. It is thus clear that the deformation of the splice region is the cardinal feature of steel-cord belt splice damages.

2.2 Principles of Monitoring and Diagnosing Splice Breakage

A wide variety of monitoring systems have been developed to detect potential faults of belt splices. Generally, all the principles and methods used in those systems can be classified as two types [1,2,3]:

- Directly detecting the impairment degree of the steel cords in the splice regions (cord break, rusting, displacement, etc.) and the condition of the bonding layer.
- Detecting the surface characteristics of the coating and its changes such as stretching deformation, blistering phenomena, surface laceration, etc., thus inferring the condition of the internal damage of splices.

Actually, the changes of the splice in length and stiffness can reflect the splice damages of all kinds and the deformation they may cause. Therefore, on condition that the F-L characteristic curve of the splice itself has been obtained, the degree of splice damage can be inferred according to the variation of the curve. Moreover, the accident of splice breakage can be also predicted and avoided according to the trend analysis of the F-L characteristic curve.

Each splice in a conveyor belt loop has its own F-L characteristic curve, but all these curves are similar in shapes and characteristics. The typical F-L characteristic curve of belt splices is shown in Fig.1, where, F denotes the tensile force acting on the splice, L the length of splice, F' the breaking tension, F_{max} the tensile force under which some steel cords begin to be drawn, F_1 and F_2 the minimum and maximum working loads respectively, L_0 the original length of the splice. Δ_{max} represents the maximum allowable deformation and l_{max} stands for the threshold alarm curve.

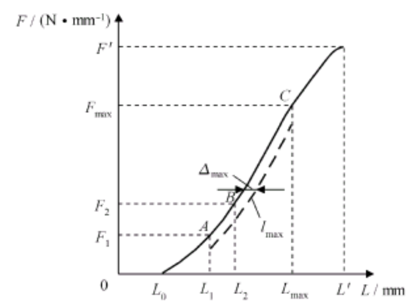

Fig.1 *F-L* characteristic curve of steel-cord belt splices

978-0-7695-3962-1/10 $26.00 © 2010 IEEE
DOI 10.1109/ICMTMA.2010.86

The maximum allowable tensile force is an important alarm threshold in monitoring the splice damages. Fig.1 shows that the curve from A to B (the normal working interval) till C is approximately a straight line. And yet, when F measures up to $F_{\max}$ under special working condition, the bonding layer in splice regions are severely undermined, some steel cords begin to be drawn and the stiffness of the splice drops visibly. So $F_{\max}$ can be defined as the maximum allowable tensile force. Generally, steel cords will not be drawn until the tensile force reaches 75% to 85% of F', the breaking tension [4]. We can thus specify 75% the value of F' as that of $F_{\max}$, the maximum allowable tensile force. And theoretically, the minimum value of F' can be estimated according to F_0, the design intensity of the belt, and η (100%, 85% or 75%), the retention coefficient of splice intensity under different splicing modes. In view of the unfavorable factors such as imperfect vulcanization of splices, splice aging effect, etc., a coefficient of safety, normally 1.5, must be taken into account as well. Thus,

$$F_{\max} = F_0 \eta \times \tfrac{1}{1.5} \times 75\% = F_0 \eta \times 50\% \qquad (1)$$

Another alarm threshold is the maximum allowable plastic deformation. As mentioned above, the deformation increasing gradually and some steel cords being drawn out can characterize all kinds of splice damages. And experiments have shown that, if the plastic deformation of a splice region reaches *10mm* or more, the splice will be badly damaged in strength and confronted with the danger of breaking at any moment [2,4]. Therefore, the maximum allowable plastic deformation $\Delta_{\max}$ is set at 10mm, and then an alarm threshold curve $l_{\max}$ of splice deformation should be set near the F-L curve, as shown in Fig.1. When the F-L curve is drifting close to or over the alarm threshold curve, an alarm signal is given.

Besides, the damage of splice finds expression not only in the deformation but also in the change in stiffness of splice, the slope of F-L curve. Especially in some particular working conditions, although the deformation is still below $\Delta_{\max}$, the splice may have been severely damaged, characterized by an obvious decrease in stiffness. So an alarm signal should also be given in this case, to be exact, when the stiffness of splice has decreased by 15% [4].

Therefore, according to the drifting trend, magnitude and velocity of the F-L characteristic curve of splice, the degree of splice damage can be monitored and the development of the damage can be forecast [4].

2.3 The Principles of Monitoring and Diagnosing the Belt Tension super-threshold

The belt conveyor, while working in some complex or particular conditions, may suffer a large impact load, which may bring about a severe damage and even a transverse breakage to the belt. Thus, an integrated protection system usually ought to contain a monitoring device of tension super-threshold.

As mentioned above, splices are the weakest links in the belt loop. Besides, compared with the other parts of the belt, splices are more liable to aging and injuries in bad working conditions. The warning threshold of tensile force is thus determined by the strength of splices. And as discussed in section 2.2, it is usually equal to $F_{\max}$, the maximum allowable tensile force.

3. Measurement of Splice Deformation

3.1 Measuring Method of Splice Deformation

In order to obtain the deformation length, the splice length must be measured before deformation and after deformation respectively, and the difference of the two measured values is the very deformation length. The Hall effect sensor is selected in this monitoring system to measure the deformation of the splice, which has the superiority of good performance, anti jamming, high measuring accuracy and high reliability.

The measuring principle applied in this paper is shown in Fig.2. Two magnets were respectively embedded in the two ends of the splice region in advance, and two Hall effect sensors are mounted under the belt, keeping a proper distance between the belt and the sensors. s_1 represents the distance between sensors a, b, which is a known quantity. And s_2, the length of splice region is the unknown variable in need of measurement. So, when the splice, together with the belt, is passing through sensors a, b at a certain uniform velocity (υ), Four impulse signals are picked up, as shown in Fig.3, where, the time intervals of the four impulse signals are denoted by t_1, t_2, t_3 respectively. It is obvious that t_1 is equal to t_3 provided that the velocity of the belt υ is uniform. And t_1, t_2 can be obtained through inputting the impulse signals into a time counter controlled by a single chip computer. Then, we get the following equations:

$$\begin{cases} s_1 = \upsilon \cdot t_1 \\ s_2 = \upsilon \cdot t_2 \end{cases} \qquad (2)$$

Thereby,

$$s_2 = \tfrac{t_2}{t_1} \cdot s_1 \qquad (3)$$

The length and the deformation of each splice can thus be obtained on the basis of this equation.

Simulation experiments and industrial application have shown that the measuring error of splice length is within $\pm 1mm$ when the flutter of the belt is no more than $4mm$ [4].

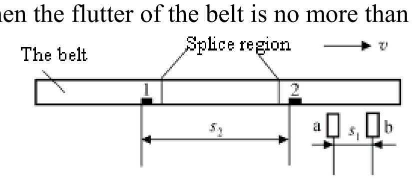

Fig.2 The measuring principle of the splice length

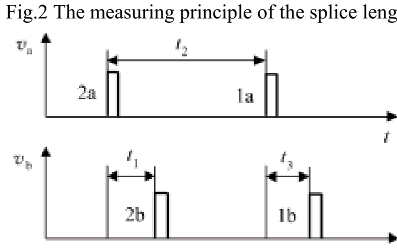

Fig.3 Output signals of Hall effect sensors

3.2 Installation of Hall Effect Sensors

While the belt conveyor being in operation, the belt experiences different tensile forces at different positions. Usually, the tensile force acting on the tight side of the belt is the largest when the belt is coming close to the driving roller; accordingly, the deformation of the splice is also the largest. So, the monitoring device is located in this area, where the maximum tensile force and the corresponding deformation of the splice can be measured simultaneously.

The installation diagram of Hall effect sensors and magnets is shown in Fig.4. In consideration of the lateral running behavior of the belt, three rectangular magnets are selected and embedded in each splice region. The length L of each magnet is defined as the difference of twice the maximum allowable deviation and the probe diameter of Hall effect sensor. If the lateral deviation of the belt is out of the allowable limits, Hall effect sensors will receive no signal, which indicates that the lateral running behavior of the conveyor belt has occurred. It is thus clear that this system can also serve to monitor the lateral running behavior of the belt [4].

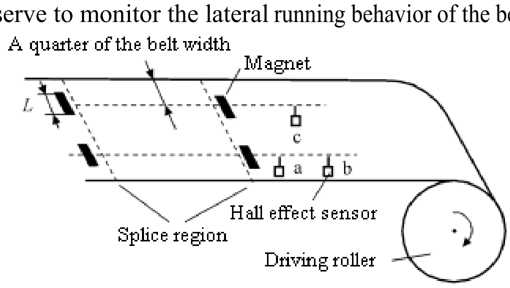

Fig.4 The installation diagram of Hall effect sensors and magnets

4 Measurement of Belt Tensions

4.1 Measuring Method of Belt Tensions

Generally, when the deflection of a steel cord belt is relatively very small, the belt may be regarded as a flexible one, that is, its cross-section bears no bending moment [5]. The force diagram of the belt is simply shown in Fig.5. *A, B* represent two supporting rollers and their span is s , with a horizontal inclination angle β . F denotes the tensile force acting on the belt. It may be assumed that the belt sustains a concentrated force *G* in the direction perpendicular to the belt at point *K*, the mid-point of the span. The belt itself weighs G_0 or sq_0g , a uniformly distributed load, here, q_0 represents the mass of the belt per unit length and g is the acceleration of gravity. The maximum deflection at point *K* is $f_{\max}$ and F_v denotes the bearing reaction of supporting roller *A*. As mentioned above, any cross-section of the belt sustains no bending moment, so the bending moments acting on the belt both at point *K* and at point *B* are all zero. Thus, there exist the following equations:

$$\sum M_K = F_v \frac{s}{2} - Ff_{\max} - \int_0^{\frac{s}{2}\cos\beta} \frac{q_0 g}{\cos\beta} x dx = 0 \tag{4}$$

$$\sum M_B = F_v s - \int_0^{s\cos\beta} \frac{q_0 g}{\cos\beta} x dx - G\frac{s}{2} = 0 \tag{5}$$

According to the two equations, $f_{\max}$ can be calculated:

$$f_{\max} = \frac{s}{4F} G + \frac{q_0 g s^2}{8F} \cos\beta \tag{6}$$

Therefore, the maximum deflection per unit span is:

$$f' = \frac{f_{\max}}{s} = \frac{1}{4F} G + \frac{q_0 g s}{8F} \cos\beta \tag{7}$$

Accordingly, we can get the following equation:

$$G = 4f'F - \frac{G_0}{2}\cos\beta \tag{8}$$

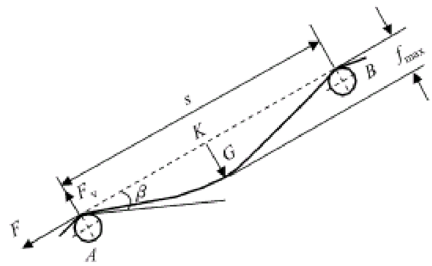

Fig.5 The force diagram of the belt

In equation (8), $G_0 \cos\beta/2$ is a known quantity, *G* and *F* are in a linear relationship ($G \propto F$) provided f' is constant. So, if we exert a pressure *G* at point *K* of the belt, producing a certain deflection f', the tensile force *F* acting on the belt may be obtained through measuring the concentrated force *G*.

It must be pointed out that although a larger f' may contribute to the enhancement of sensitivity, it is unadvised to excessively increase the value of f' . Because, if f' is too large, the belt can no longer be approximately regarded as a flexible one and those equations will not be fit for this case any longer. Usually, f' ought to be no more than 2%.

A simulation device has been established to verify the feasibility and reliability of the measuring method of belt tensions, as shown in Fig.6. Experimental results have shown that when f' is constant, *G* and *F* are in a good linear relationship and the measured linear coefficient is also approximately equal to $4f'$, the theoretic coefficient [4].

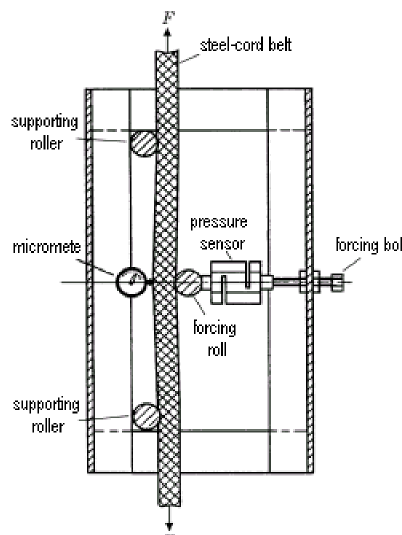

Fig.6 The simulation device for measuring the tension of the belt

4.2 The measuring Device of Belt Tensions

As mentioned in 3.2, the tensile force acting on the tight side of the belt is usually the largest when the belt is coming close to the driving roller, so the measuring device of belt tensions should be mounted at this location.

The fundamental components of the measuring device include two supporting rollers (A, B) with a proper span and a forcing roller C, which is fixed on the opposite side of the belt at the mid-point of the span. To produce a certain deflection, a pressure is exerted on the belt through the forcing roller C, which can be measured by the pressure sensor mounted at the two ends of the forcing roller C. The installation diagram of the tension-monitoring device is shown Fig.7 and the structure of this real device is quite similar to that of the simulation device shown in Fig.6. The measurement range of the sensor is determined by f' and the maximum allowable tension F, that is, selected according to the calculated value of equation (8). All the rollers adopted in this system are small standard mining rollers, whose strengths have been checked according to the pressure acting on the axles of the rollers [4].

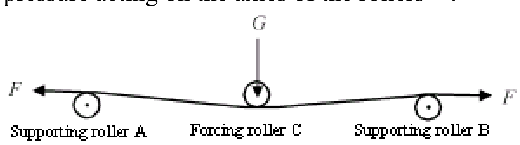

Fig.7 The installation diagram of the tension-monitoring device

5. Computer Real-time Monitoring System

Based on the above-mentioned principles and methods, a computer real-time monitoring system has been developed, which is mainly composed of an explosion-proof DC voltage-stabilized source, a host processor, a set of device for measuring the splice deformation, a set of device for measuring belt tensions, an alarm display screen and an audible-visual annunciator. The host processor adopted in this system is 80C196KB, a 16-bit microprocessor with four high-speed input (HSI) channels and eight A/D interfaces, which is capable of picking multiplex impulse signals and analogue signals. The impulse signals, coming from the Hall effect sensors used to measure the splice deformation, go through a shaping circuit first and are then input into the HSI interfaces; the analogue signals from the pressure sensors used to measure the splice tension go through a summing amplifier, a low-pass filter and a 50Hz trap circuit successively, and then are fed into A/D interfaces. Fig.8 has depicted the structural diagram of this system.

5.1 Monitoring and diagnosis of the splice damage

While the impulse signals being input into the HSI interface, their hitting time is recorded by the 80C196 simultaneously. Then the length of the splice, L, can be calculated according to equation (3). The corresponding tensile force F can be obtained through averaging those measured values from the A/D interfaces during the period of the belt splice passing. However, in order to improve the measuring accuracy, each effective value is actually the weighted means of four groups of measured values. The reference F-L curves of all the splices in a belt loop are drawn after a certain period of trial operation and calibration test, and then, the stiffness parameter k can be calculated by the method of linear regression. The damage degree of the splice in operation can thus be monitored and predicted by means of threshold analysis and trend analysis.

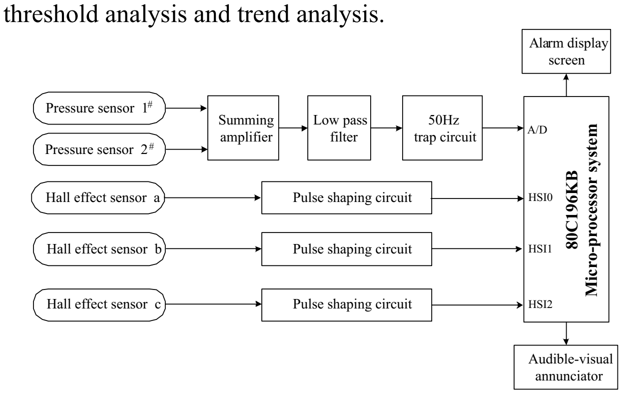

Fig.8 The structural diagram of the computer real-time monitoring system

5.2 Monitoring of tension super-threshold

The sensitivity coefficients of the pressure sensor and the converter circuits is calibrated through experiments, so the pressure G can be obtained through the conversion of the average of the measured voltages from A/D interfaces during a certain period, and then the tensile force F can be calculated according to equation (8).

There might be a small linearity error between the calculated value of F and its true value because of the inaccuracy of f'. However, being a kind of steady systematic error, it has no effect on the fault diagnosis of splice damages. On the other hand, because the safety factor of belt design is usually 10, even if the splice is in the weakest splicing mode (η=0.75), the maximum allowable tensile force $F_{\max}$ is still over 3.75 times the maximum working load (see equation (1)). So the measured error of F does not effect the monitoring of tension super-threshold, either. In a practical monitoring system, usually, $F_{\max}$ can be set as 2~3 times the maximum of measured tensile force in order to avoid the damage to the belt caused by large abnormal loading.

6. Conclusions

This findings introduced in this paper is the outcome of the project "Research on real-time monitoring system for the working conditions of steel-cord belt conveyor ", which is sponsored by the former Department of China Coal Industry. The new method of monitoring the steel-cord belt splice breakage and tension super-threshold, which is established on the basis of the measurement and analysis of the F-L characteristic curve of steel-cord belt splices, has turned out to be a breakthrough in this field. And the real-time monitoring system developed according to this method has been successfully applied in Xishan coal board, China.

REFERENCES

[1] Harrison A.: Wear Profile measurement of the rubber covers of steel-cord belts [J]; Coal Miner, 1981(3), pp. 38-41.
[2] Harrison A.: Review of conveyor belts monitoring research in Australia [J]; Bulk Solids Handling; 1985(6), pp.1181-1184.
[3] Harrison A.: Monitoring system for steel-reinforced conveyor belts [J]; Journal of Engineer for Industry; Transactions of the ASME, 1986(5), pp. 148-153.
[4] Huang Min: Method for Real-time Monitoring and Fault Diagnosis of Steel-cord Belt conveyors [D]; China University of Mining and Technology, Xuzhou, 1997.
[5] Huang Wanjie: Design of Mine transporting Machines; Publishing House of Northeast Institute of Technology (Shenyang); 1990, pp.32-33.